Femtosecond investigation of the hot-phonon effect in GaAs at room temperature

P. Langot, N. Del Fatti,* D. Christofilos,† R. Tommasi,‡ and F. Vallée
Laboratoire d'Optique Quantique du Centre National de la Recherce Scientifique, Ecole Polytechnique, 91128 Palaiseau Cédex, France
(Received 15 April 1996; revised manuscript received 15 July 1996)

Slowing down of the hot electron-lattice thermalization by generation of nonequilibrium phonons (hot-phonon effect) is investigated in GaAs at room temperature using high-sensitivity femtosecond single- and double-wavelength absorption saturation techniques. Measurements were performed for different amplitudes of the hot-phonon effect by changing either the individual excess energy of the photoexcited carriers or their density in the range 7×10^{15}–4×10^{17} cm^{-3}. After an initial regime dominated by nonequilibrium LO-phonon k-space redistribution, the long-time delay ($\geqslant$3 ps) electron thermalization is found to occur with a characteristic time of ~1.9 ps, independent of the total energy initially injected into the carriers and essentially reflecting the LO-phonon energy relaxation. This is in agreement with numerical simulations of the coupled carrier-phonon relaxation dynamics, indicating that energy transfers to holes are responsible for this slight reduction of the thermalization time compared to the LO-phonon lifetime (identified with the dephasing time $T_2/2\sim2.1$ ps). [S0163-1829(96)02244-8]

I. INTRODUCTION

Carrier-lattice energy exchanges are essentially mediated by LO phonons in polar semiconductors. In these systems, the excess energy of carriers out of equilibrium with the lattice is first transferred to small momentum LO phonons, which subsequently decay into large wave-vector phonons at the edge of the Brillouin zone via the crystal potential anharmonicity. The intrinsic lifetime of the LO phonons being generally much longer than their interaction time with carriers, they can be driven out of equilibrium during electron relaxation.[1–5] This bottleneck effect slows down the electron-lattice thermalization, the nonequilibrium phonons acting as an energy reservoir (hot- or cold-phonon effect). This effect is *a priori* strongly dependent on the LO-phonon relaxation dynamics, which is thus expected to eventually govern the electron thermalization.[5–7]

The hot-phonon effect has been extensively investigated in bulk and low-dimensionality semiconductors, by measuring either the density dependence of the thermalization rate of hot carriers by time-resolved luminescence[4,8–11] or by detecting the induced phonon overpopulation using time-resolved spontaneous Raman scattering.[12–15] However, most of the carrier thermalization measurements have been performed at low-temperature and electron-lattice thermalization times τ_e largely exceeding the phonon lifetime τ_{LO} have been measured. This absence of direct correlation between τ_e and τ_{LO} can be partly ascribed to the influence of acoustic phonons and to the fact that a large part of the energy is stored into the electron gas.[6] Furthermore, because of their low equilibrium occupation number, the zone edge phonons into which the nonequilibrium LO phonons relax can also be significantly driven out of equilibrium, resulting in a second bottleneck effect by slowing down the LO-phonon energy relaxation.[16–20] For high carrier densities, intervalley scattering,[10,21,22] screening of the Fröhlich interaction and plasmon-phonon hybridization[23–25] further complicate interpretation of the measurements. Investigation of the hot-phonon effect on electron thermalization has been hampered by these effects, and a direct observation has been reported only recently in low-temperature grown GaAs.[26]

We have studied the hot-phonon effect in GaAs at room temperature by precisely measuring hot electron cooling on a picosecond time scale using femtosecond one- and two-wavelength absorption saturation techniques. Although the absolute transient carrier temperature cannot be determined, its relative changes can be very precisely measured permitting an accurate analysis of carrier thermalization with the lattice. We demonstrate that in the weak perturbation regime (i.e., for carrier density $\leqslant4\times10^{17}$ cm^{-3} and initial electron excess energy $\leqslant3\hbar\omega_{\mathrm{LO}}$) the long-term ($t\geqslant1$ ps) electron thermalization is directly related to the LO-phonon relaxation dynamics.

Numerical simulations of the coupled carrier-phonon relaxation dynamics and a simple rate equation model are presented in Sec. II and compared to experiments in Sec. IV after description of our high repetition rate femtosecond two-color system in Sec. III.

II. THEORETICAL MODELS

A. Numerical simulations

In these studies we are interested in the carrier relaxation dynamics after many scattering events. Coherent effects will thus be neglected and the carrier system will be simply described by the wave-vector-dependent occupation numbers, f_i, of the different bands. The time evolution of the nonequilibrium distributions can then be calculated by numerically solving the coupled carrier-phonon Boltzmann equations:[3]

$$\frac{df_i(\mathbf{k})}{dt}=\sum_j\left(\frac{df_i(\mathbf{k})}{dt}\right)_j+\left(\frac{df_i(\mathbf{k})}{dt}\right)_{\mathrm{phonons}}+g_i(\mathbf{k},t), \tag{1}$$

$$\frac{dn_{\mathrm{LO}}(\mathbf{q})}{dt}=\left(\frac{dn_{\mathrm{LO}}(\mathbf{q})}{dt}\right)_{\mathrm{el}}+\left(\frac{dn_{\mathrm{LO}}(\mathbf{q})}{dt}\right)_{\mathrm{lh}}+\frac{n^0_{\mathrm{LO}}-n_{\mathrm{LO}}(\mathbf{q})}{\tau_{\mathrm{LO}}},$$

 © 1996 The American Physical Society

where i,j stand for the electron (el), heavy-hole (hh), and light-hole (lh) bands, n_{LO} is the transient wave-vector-dependent LO-phonon occupation number and g_i is a photoinjection function determined by the pump pulse. Coupling of the LO phonons with the other lattice modes via the crystal potential anharmonicity is described in the relaxation time approximation (n^0_{LO} is the equilibrium value of n_{LO} at room temperature). As the LO phonons are perturbed over a small central part of the Brillouin zone, dispersion of the crystal anharmonicity and of the density of the phonon states into which they relax are negligible and a constant LO-phonon lifetime τ_{LO} has thus been used.

The carrier-carrier $(df_i/dt)_j$ and carrier-phonon $(df_i/dt)_{\mathrm{phonons}}$ scattering rates are identical to those extensively discussed by many authors for isotropic parabolic conduction and valence bands[3,27–30] and will not be given here. All carrier-carrier scattering processes have been included (except those inducing intervalence band scattering) using static screening by carriers of identical or smaller mass.[10,29,31] Dynamic screening in the plasmon pole approximation has been used for screening of the LO-phonon polar interactions with electron and light holes.[32] Nonpolar TO- and LO-phonon–hole interactions and statically screened polar LO-phonon–hole scattering have been considered for hh intraband processes and intervalence band processes.

The transient modification of the phonon distribution has been taken into account only for LO phonons interacting with electrons and light-holes but has been neglected in computing the heavy-hole–LO-phonon scattering rates and for TO phonons. This is justified by the fact that because of their larger mass, hh interact with large momentum (i.e., large density of states) optical phonons over a k-space domain that is strongly broadened by the hh band anisotropy. In contrast to electrons and lh, hh thus interact with a high heat capacity phonon reservoir. Furthermore, for a pump wavelength $\lambda_{\mathrm{pp}} \geqslant 780$ nm, holes are photoexcited with an average energy smaller than the thermal one (E_{th}). They thermalize with, on the average, absorption of less than one phonon per hole, which only weakly depletes the phonon distribution, in agreement with the absence of any phonon underpopulation effect on hole heating in GaAs.[33–35]

The electron distributions calculated for different time delays after photoexcitation with a 100-fs Gaussian pulse at $\lambda_{\mathrm{pp}}=810$ nm ($\hbar\omega_{\mathrm{pp}} \sim 1.53$ eV) are shown in Fig. 1 for a carrier density of 1×10^{17} cm^{-3}. The electron distribution internally thermalizes in a few hundred femtoseconds[32] and subsequently cools down to the lattice temperature on a picosecond time scale. The corresponding time evolution of the LO-phonon distribution is shown in Fig. 2 exhibiting a large overpopulation built up with a dynamics strongly dependent on the phonon wave vector q_{LO}.[3,21] Multiple LO-phonon absorption and emission by the electrons redistribute the excess energy in the phonon system tending to internally thermalize it.[6,21] For long time delay ($t \geqslant 4$ ps), the occupation numbers of the small q_{LO} phonons are comparable (i.e., a quasitemperature is established) and they return to their equilibrium value with a time constant close to τ_{LO} (Fig. 2, inset).

B. Simplified rate equation model

In this regime, as the electron gas strongly interacts with the small q_{LO} phonons ($0.7\times10^6 \leqslant q_{\mathrm{LO}} \leqslant 2\times10^6$ cm^{-1}), its temperature T_e is expected to follow their quasitemperature. The electron-lattice thermalization can then be described by a simple rate equation model for energy exchanges of the coupled electron–LO-phonon system with the lattice and the holes:

$$\frac{\partial(\Delta E_e+\Delta E_{\mathrm{LO}})}{\partial t} = -\frac{\Delta E_{\mathrm{LO}}}{\tau_{\mathrm{LO}}} - \delta E_{e\text{-}h} - \delta E_{\mathrm{LO}\text{-}h}, \qquad (2)$$

where ΔE_e and ΔE_{LO} are the transient excess energy $[\Delta E_{e,\mathrm{LO}}=E_{e,\mathrm{LO}}(t)-E^{\mathrm{th}}_{e,\mathrm{LO}}]$ stored in the electron and phonon subsystems. $\delta E_{e\text{-}h}$ and $\delta E_{\mathrm{LO}\text{-}h}$ are, respectively, the time-dependent electron and LO-phonon energy loss rates to the holes. Assuming that the perturbed small momentum LO

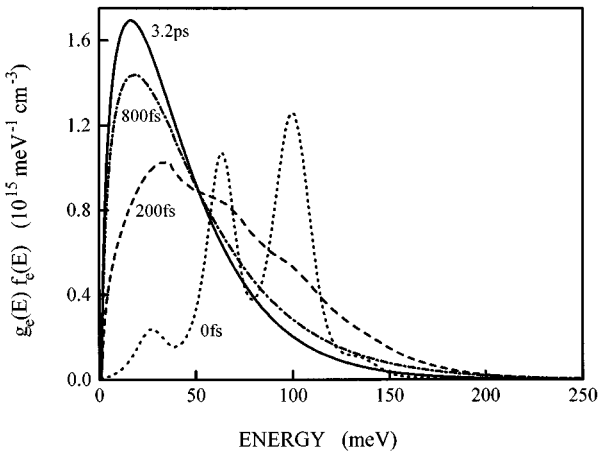

FIG. 1. Calculated transient electron distribution $f_e(E)$ times the density of electron states $g_e(E)$ for different time delays after carrier photoexcitation in GaAs at 295 K. The temporal origin is the maximum of the 100-fs pump pulse. The pump photon energy is 1.53 eV ($\lambda_{\mathrm{pp}} \sim 810$ nm) and the carrier density 1×10^{17} cm^{-3}.

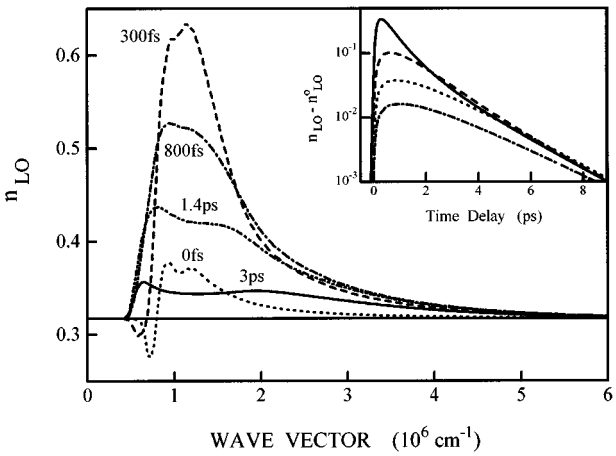

FIG. 2. Calculated occupation number n_{LO} of the LO phonons as a function of their wave vector q_{LO} for different time delays after carrier photoexcitation (the excitation conditions are identical to those of Fig. 1). The horizontal line represents the equilibrium phonon occupation number at room temperature (n^0_{LO}). The inset shows the time dependence of the excess occupation number, $n_{\mathrm{LO}}-n^0_{\mathrm{LO}}$, on a logarithmic scale, for $q_{\mathrm{LO}}=1.1\times10^6$ cm^{-1} (full line), 2×10^6 cm^{-1} (dashed line), 3×10^6 cm^{-1} (dotted line), and 4×10^6 cm^{-1} (dash-dotted line).

phonons are internally thermalized and in equilibrium with the electron gas, the evolution of their common excess temperature $\Delta T_e = T_e - T_l$ ($T_l = 295$ K) is given by

$$\frac{\partial \Delta T_e}{\partial t} = -\frac{\Delta T_e}{(1 + C_e/C_{\mathrm{LO}})\tau_{\mathrm{LO}}} - \frac{\delta E_{e\text{-}h} + \delta E_{\mathrm{LO}\text{-}h}}{C_e + C_{\mathrm{LO}}}, \quad (3)$$

where C_e and C_{LO} are, respectively the heat capacity of the electron gas and of the LO phonons coupled with it. For nonzero temperatures, momentum and energy conservation do not impose a precise cutoff for the LO-phonon wave vector and C_{LO} is thus not precisely defined.[7] However, for moderate carrier densities, C_{LO} is much larger than C_e (Ref. 20) [$C_{\mathrm{LO}}/C_e > 10$ for $\rho = 1\times10^{17}$ cm^{-3}, limiting q_{LO} to the momentum space region 0–5×10^6 cm^{-1} (Fig. 2)]. This is in agreement with numerical computation of ΔE_{LO} and ΔE_e showing that most of the total transient excess energy, $\Delta E_e + \Delta E_{\mathrm{LO}}$, is stored in the LO-phonon subsystem for time longer than ~1 ps (~90% after 3 ps).

Neglecting interactions with holes, ΔT_e is thus expected to decay exponentially with a time constant $\tau_e = \tau_{\mathrm{LO}}(1 + C_e/C_{\mathrm{LO}})$, close to τ_{LO} in our experimental conditions. This is in contrast with the high-density and low-temperature measurements for which C_e/C_{LO} can be much larger than one, leading to large deviations of τ_e from τ_{LO}. We have demonstrated this correlation between the intrinsic LO-phonon lifetime and the long-term electron-lattice thermalization time by performing two-wavelength femtosecond absorption saturation measurements.

III. EXPERIMENTAL SYSTEM

The two pulses are created by frequency conversion of a Kerr-lens mode-locked Ti:Al_2O_3 laser. The laser is operated at 800 nm with an average power of 1.6 W and a pulse duration of ~50 fs. The pulse train is coupled into a 5.5-cm-long, 3.9-μm core diameter single mode optical fiber where self-phase modulation strongly broadens the original spectrum from ~14 to ~130 nm full width at half maximum. The output of the fiber is split into two parts, which are temporally compressed and spectrally filtered using two identical systems consisting of two diffraction gratings separated by a unity magnification telescope. Wavelength selection of nearly Gaussian pulses is achieved by means of slits placed out of the Fourier planes.[5,36] Their widths are adjusted to produce 100-fs transformed limited pulses with a maximum power of ~20 mW. The two beams are cross polarized and are sent into a standard pump-probe arrangement. The pump beam was focused to a focal spot 50 μm in diameter and the probe beam to a smaller focal spot of 35 μm to limit the effect of excitation inhomogeneity. The pump beam was chopped at 1.5 kHz and a standard lock-in differential detection technique was utilized. Experiments were performed at room temperature in a 0.2-μm-thick intrinsic GaAs sample with $Al_{0.6}Ga_{0.4}As$ cladding layers and antireflection coating.

In absorption saturation measurements, the relaxation dynamics of the photoexcited carriers is investigated by monitoring the transmission change, $\Delta T/T = [T(\rho) - T(0)]/T(0)$, of a time delayed probe pulse (ρ is the carrier density). For the probe photon energies $\hbar\omega_{\mathrm{pr}}$ used here $\Delta T/T$ is proportional to the change $\Delta\alpha$ of the free carrier related sample absorption:

$$\alpha(\hbar\omega_{\mathrm{pr}}, \rho) = \alpha_0 \sum_v \mu_v^{3/2} C_v(\hbar\omega_{\mathrm{pr}}, \rho)\sqrt{\hbar\omega_{\mathrm{pr}} - E_g(\rho)} \times [1 - f_e(k_{\mathrm{pr}}^v) - f_v(k_{\mathrm{pr}}^v)], \quad (4)$$

where the summation is performed on the hh and lh bands. μ_v is the reduced electron-hole mass, and $k_{\mathrm{pr}}^v = \sqrt{2\mu_v[\hbar\omega_{\mathrm{pr}} - E_g(\rho)]}/\hbar$ the wave vector of the probed states. Change of the sample absorption after carrier photoexcitation results from band filling (BF) and modification of the Coulomb enhancement factor C_v, and renormalization of the band gap E_g.[3,34] In our experimental conditions, BF dominates and the transient absorption is related to the time-dependent carrier distributions and hence to their temperature when the carrier subsystems are internally thermalized.

Because of the high stability and high repetition rate of our system, noise levels for $\Delta T/T$ measurement as low as a few 10^{-6} can be achieved with different pump and probe wavelengths. For single-wavelength measurements, the pulse train from the Ti:sapphire oscillator is directly sent into the same pump-probe setup and the noise level is then reduced to a few 10^{-7}. The carrier dynamics can thus be followed with a very high precision, an electron temperature change ΔT_e of ~0.5 K corresponding for instance to a change of $\Delta T/T$ of 5×10^{-6} for $\rho = 1\times10^{17}$ cm^{-3} and $\lambda_{\mathrm{pr}} = 810$ nm ($\hbar\omega_{\mathrm{pr}} \sim 1.53$ eV).

Measurements were performed for electrons photoexcited with an initial energy smaller than the threshold for L-valley scattering. Even in these conditions, for large carrier densities, fast electron-electron collision can strongly broaden the initial distribution, leading to a significant intervalley transfer that can modify electron relaxation.[21,22] Moderate densities and initial electron energies were thus used here to limit that effect. For instance, for a carrier density of 1×10^{17} and a pump wavelength of 780 nm our numerical model shows that during electron relaxation, less than 0.6% of the electrons can reach an energy larger than the threshold for scattering into the L valley.

IV. RESULTS AND DISCUSSION

The measured normalized transmission changes $\Delta T/T$ are shown in Fig. 3 for identical pump and probe wavelengths $\lambda_{\mathrm{pp}} = \lambda_{\mathrm{pr}} \sim 810$ nm ($\hbar\omega_{\mathrm{pp}} = \hbar\omega_{\mathrm{pr}} \sim 1.53$ eV) corresponding to excitation of electrons (holes) with an initial average energy $E_{\mathrm{ex}}^e \sim E_{\mathrm{th}} + 43$ meV ($E_{\mathrm{ex}}^h \sim E_{\mathrm{th}} - 14$ meV). The measured temporal behavior is similar to that previously reported with a fast transient peak around $t_d = 0$, which has been attributed to a hole burning effect.[38,39] As the small-time delay dynamics ($t_d < 1$ ps) has been extensively studied,[37–39] it will not be discussed here and we will focus on the long-time delay signal that *a priori* reflects both electron- and hole-lattice thermalizations. In our experimental conditions, the electron contribution dominates the long delay signal, since the band filling (BF) effect is about two times larger for electrons than for holes for $\hbar\omega_{\mathrm{pr}} = 1.53$ eV and hole-lattice thermalization (hole heating here) is completed in less than 1 ps.[34]

The electron and hole contributions can be further separated by performing measurements for the same probe wavelength (810 nm) and carrier density but for different pump wavelengths, to change the initial energy content of the car-

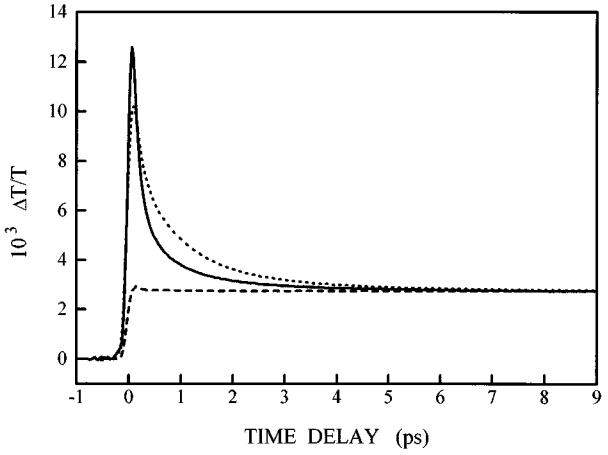

FIG. 3. Measured transient differential transmission $\Delta T/T$ in GaAs at 295 K for a probe wavelength of 810 nm and a carrier density of 1×10^{17} cm^{-3}. The pump wavelength is 810 nm (full line), 780 nm (dotted line), and 835 nm (dashed line).

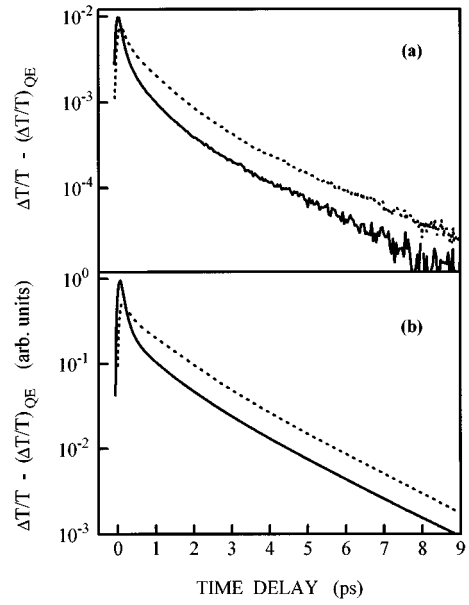

FIG. 4. Measured (a) and calculated (b) transient transmission difference $DT=\Delta T/T-(\Delta T/T)_{\mathrm{QE}}$ on a logarithmic scale [$(\Delta T/T)_{\mathrm{QE}}$ is the long delay $\Delta T/T$ measured for $t=15$ ps]. The carrier density is 1×10^{17} cm^{-3} and the pump wavelength 810 nm (full line) and 780 nm (dotted line). The probe wavelength is 810 nm.

riers. For $\lambda_{\mathrm{pp}}\sim835$ nm ($\hbar\omega_{\mathrm{pp}}\sim1.485$ eV) the nonequilibrium electrons are photoexcited with $E^e_{\mathrm{ex}}\sim E_{\mathrm{th}}+8$ meV close to the thermal energy while the initial average energy of the holes is reduced of ~10 meV compared to that for $\lambda_{\mathrm{pp}}\sim810$ nm ($E^h_{\mathrm{ex}}\sim E_{\mathrm{th}}-24$ meV). However, the transient transmissivity reaches its equilibrium value on a much shorter time scale as shown in Fig. 3 consistent with the smaller initial excess energy of the electrons.[40] In contrast, when holes are photoexcited with an initial energy close to E_{th} (i.e., $\lambda_{\mathrm{pp}}\sim780$ nm, $\hbar\omega_{\mathrm{pp}}\sim1.59$ eV) a slowly decaying signal is observed with a larger amplitude than for $\lambda_{\mathrm{pp}}\sim810$ nm (Fig. 3), consistent with higher energy injection into the electron system ($E^e_{\mathrm{ex}}\sim E_{\mathrm{th}}+89$ meV). This large dependence of the $\Delta T/T$ temporal behavior on the initial excess energy of the electrons confirms that the measured slow thermalization can be ascribed to hot-electron cooling and that hole thermalization dynamics plays a minor role in the measured transient response.

When electrons are photoexcited with a significant excess energy relative to E_{th} (i.e., $\lambda_{\mathrm{pp}}\sim780$ or 810 nm), $\Delta T/T$ slowly reaches a plateau, indicating that the electrons are still hotter than the lattice for times as long as 8 ps (Fig. 3). This slow thermalization is evidenced in Fig. 4 where the difference, $DT=[(\Delta T/T)-(\Delta T/T)_{\mathrm{QE}}]$, between $\Delta T/T$ and its quasiequilibrium (QE) value $(\Delta T/T)_{\mathrm{QE}}$ has been plotted on a logarithmic scale as a function of the probe time delay for $\lambda_{\mathrm{pr}}\sim810$ nm [$(\Delta T/T)_{\mathrm{QE}}$, which corresponds to carrier-lattice thermal equilibrium, has been measured for $t=15$ ps]. The amplitude of DT is related to the excess occupancy of the probed electron states $f_e(T_e)-f_e(295\ \mathrm{K})$ and hence for small system perturbations is proportional to the excess temperature ΔT_e of the electron gas when it is internally thermalized (i.e., for $t\geqslant500$ fs). The DT decay thus directly reflects the electron cooling dynamics.

A slow DT decay is observed for $t>1$ ps with an almost monoexponential behavior for $t>3$ ps with a time constant of $\tau_e\sim1.9$ ps comparable with the LO-phonon dephasing time in GaAs at room temperature (~2.1 ps). This slow thermalization, with a time constant close to that observed for cold electron heating,[5] is in good agreement with that predicted by the rate equation model (3). It has to be noted that for short time delay ($t\leqslant3$ ps) a faster decay time is observed because of nonequilibrium LO-phonon momentum space diffusion [internal thermalization of the LO-phonon system (Fig. 2)] which is equivalent to increasing C_{ph} with time in our simple model.

The DT amplitudes measured for different pump wavelengths are directly comparable for the same probe wavelength and photoexcited carrier density [$(\Delta T/T)_{\mathrm{QE}}$ is thus constant] permitting us to compare the electron excess temperature for different excitation conditions. As the pump wavelength decreases from 810 to 780 nm, the long-time delay DT amplitude (and thus ΔT_e) is measured to increase by a factor of 2.1 (Fig. 4). As the heat capacity of the coupled electron and phonon system is almost unchanged, this ΔT_e rise simply reflects the increase of the energy injected into the system by more than a factor of 2 (the average excess energy ΔE_e of the photoexcited electrons increases from 43 to 89 meV). The measured decay times for $t>3$ ps are, however, identical ($\tau_e=1.9\pm0.1$ ps) as they are mainly determined by the LO-phonon anharmonic decay and thus independent of the excess energy stored in the electron and LO-phonon coupled systems (3).

The experimental results are in very good agreement with the transient transmission changes calculated from the computed carrier distributions using $\tau_{\mathrm{LO}}=2.1$ ps [Fig. 4(b)]. The computed $\Delta T/T$ neglecting the hot-phonon effect [i.e., neglecting modifications of n_{LO} by imposing $n_{\mathrm{LO}}(q)=n^0_{\mathrm{LO}}$ in the simulations] shows a fast decay, which is only weakly sensitive to the screening model (dotted line in Fig. 5). Our calculations show that for intermediate time delays ($1\leqslant t\leqslant3$ ps), the electron thermalization dynamics is dominated by momentum space diffusion of the nonequilibrium LO phonons (Fig. 2). As the electron gas strongly interacts with the small q_{LO} phonons ($0.7\times10^6\leqslant q_{\mathrm{LO}}\leqslant2\times10^6$

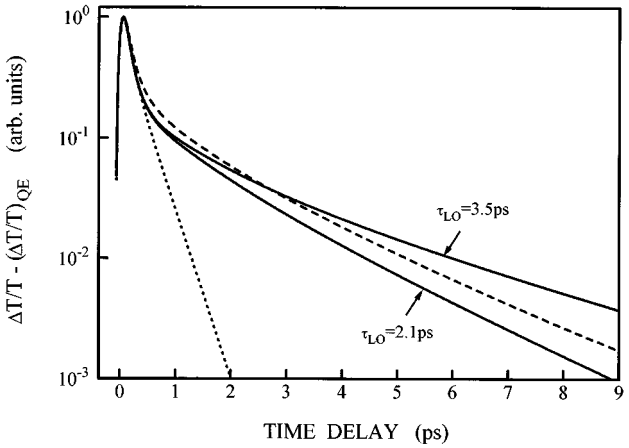

FIG. 5. Calculated differential transmission difference $DT=\Delta T/T-(\Delta T/T)_{QE}$ on a logarithmic scale [$(\Delta T/T)_{QE}$ is the long delay $\Delta T/T$]. The carrier density is 1×10^{17} cm^{-3} and the pump and probe wavelengths 810 nm. The full lines are calculated with the full numerical model with $\tau_{LO}=2.1$ ps (lower curve) and 3.5 ps (upper curve). The dashed and dotted lines are computed neglecting, respectively, energy exchanges with holes (for $\tau_{LO}=2.1$ ps) and the hot-phonon effect.

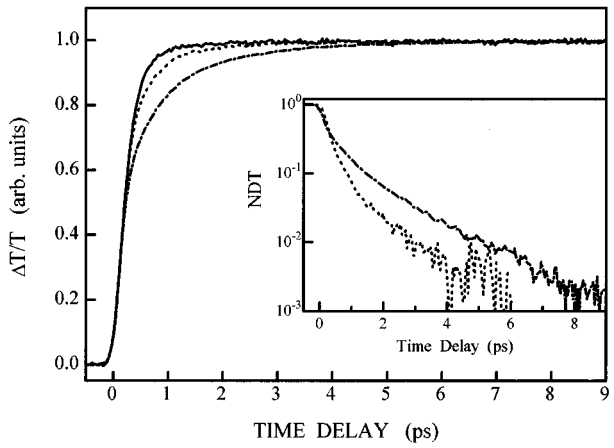

FIG. 6. Normalized transient differential transmission $\Delta T/T$ in GaAs at 295 K for pump and probe wavelengths of, respectively, 780 and 850 nm. The carrier density is 7×10^{15} cm^{-3} (full line), 3×10^{16} cm^{-3} (dotted line), and 4×10^{17} cm^{-3} (dash-dotted line). The inset shows the time dependence of the corresponding normalized transient transmission difference $[(\Delta T/T)_{QE}-\Delta T/T]/(\Delta T/T)_{QE}$ on a logarithmic scale for the two higher densities [$(\Delta T/T)_{QE}$ is the long delay $\Delta T/T$ measured for $t=15$ ps].

cm^{-1}), its temperature decreases with the energy stored in these phonon modes. The importance of this effect diminishes with time as the nonequilibrium phonon distribution tends to thermalize and the decay is eventually governed by the LO-phonon lifetime.

The calculated and measured long-term decay times are identical (Fig. 4) and close to the long-time decay of the LO-phonon overpopulation (Fig. 2). The computed τ_e is smaller than τ_{LO} because of energy exchanges of the coupled electron-phonon system with the holes. Switching off the electron-hole and nonequilibrium phonon-hole interactions in the numerical simulations results in a long-term relaxation time of 2.2 ps, slightly longer than τ_{LO} (Fig. 5) in agreement with the prediction of the rate equation model for $\delta E_{LO\text{-}h}=0$ and $\delta E_{e\text{-}h}=0$ [Eq. (3)]. Energy transfer to the holes thus compensates for the increase of τ_e compared to τ_{LO} due to the heat capacity effect (3), introducing additional relaxation channels for the nonequilibrium LO phonons by indirectly coupling them with zone center TO phonons and with large wave vector LO phonons.

In our simulations, the intrinsic LO-phonon lifetime has been identified with the dephasing time $T_2/2$, which has been precisely determined in GaAs using time-resolved coherent anti-Stokes Raman scattering (CARS) (Ref. 41) ($\tau_{LO}=T_2/2$). Although pure dephasing processes can lead to a dephasing time significantly shorter than the lifetime, these are unlikely in good quality crystals and the dephasing time has been interpreted in terms of population relaxation in GaAs.[41] The dephasing time has been used rather than the lifetime measured using time-resolved spontaneous Raman scattering [~3.5 ps (Ref. 13)] because of the possible influence of the photoexcited carriers on the measured τ_{LO} and the higher precision of the room-temperature determination of T_2. Furthermore, the results of similar calculations performed using a larger value for τ_{LO} (3.5 ps) exhibit a much longer decay time as shown in Fig. 5.

The amplitude of the hot-phonon effect on electron cooling is also very well reproduced as is its dependence on the initial energy of the photoexcited electrons (Fig. 4). The computed DT increases by a factor of 2 as the pump wavelength is reduced from 810 to 780 nm, in close agreement with the measured change. Note that the electron excess temperature ΔT_e is computed to be only 14 K for a time delay of 3 ps and $\lambda_{pp}=810$ nm.

Measurements were also performed for probing small energy electronic states ($E^e<50$ meV). The occupation number of these states increases with decreasing the electron gas temperature and hence $\Delta T/T$ due to BF increases as the system thermalizes (Fig. 1). This is exemplified in Fig. 6 for $\lambda_{pp}=780$ nm and $\lambda_{pr}=850$ nm and three carrier densities (7×10^{15}, 3×10^{16}, and 4×10^{17} cm^{-3}). The signal rise time strongly increases with density as a consequence of a larger hot-phonon effect. The long-term thermalization shows a similar exponential behavior with the same characteristic time of ~1.9 ps (inset of Fig. 6). Note that for this probe wavelength, the contribution due to filling of the conduction band is about 10 times larger than for the valence band,[5] further confirming that the observed behavior is dominated by the electron thermalization dynamics.

The various measurements performed in the carrier density range 3×10^{16}–4×10^{17} cm^{-3} for $\lambda_{pp}=810$ and 780 nm show the same behavior with no variation of τ_e with carrier density within experimental accuracy ($\tau_e=1.85\pm0.15$ ps). This is in agreement with the numerically computed weak modification of τ_e from 1.85 ps for $\rho=3\times10^{16}$ cm^{-3} to 1.95 ps for $\rho=4\times10^{17}$ cm^{-3}. The increase of the electron heat capacity might result in an increase of τ_e [Eq. (3)]. This effect is actually compensated by the increase of the energy loss rate of the coupled electron-phonon system to the holes.

The amplitude of the slow component decreases with carrier density (Fig. 6), which is consistent with injection of less energy into the system, similarly to what has been observed by changing the initial energy of the individual carrier for a

fixed density (Fig. 4). A simple quantitative comparison of the transient electron temperatures is difficult here since it requires normalization of the measured data [$(\Delta T/T)_{QE}$ is different for the different densities]. The measured reduction by a factor ~3.1 of the normalized differential transmission [$=[(\Delta T/T)_{QE}-\Delta T/T]/(\Delta T/T)_{QE}$] for decreasing the carrier density from 4×10^{17} to 3×10^{16} cm^{-3} is consistent with the computed one of 2.3.

V. CONCLUSION

The thermalization of hot electrons with the lattice has been precisely investigated in bulk GaAs at room temperature in a regime where the heat capacity of the LO phonons coupled with the electrons largely exceeds that of the electron gas. Measurements were performed using a high-sensitivity single- or double-wavelength absorption saturation techniques that permit observation of relative temperature changes of less than 1 K. After internal thermalization of the electron gas, a slow decay of the electron temperature is observed ($t\geqslant1$ ps) with a quasiexponential long-term ($t\geqslant3$ ps) evolution with a time constant $\tau_e\sim1.9$ ps, close to the room temperature LO-phonon dephasing time (~2.1 ps). Similar results were obtained by varying the pump photon energy and the carrier density (in the range from 2×10^{16} cm^{-3} to 4×10^{17} cm^{-3}), with the amplitude of the long-term component directly related to the excess energy initially injected into the electrons. The long-term thermalization time has, however, been found to be almost independent of the excitation conditions ($\tau_e=1.85\pm0.15$ ps), as it essentially reflects the LO-phonon energy decay.

These experimental results are in very good agreement with numerical simulations of the coupled carrier-phonon dynamics when the LO-phonon lifetime is identified with the previously measured dephasing time (2.1 ps). In our experimental conditions [room temperature and moderate carrier densities ($<5\times10^{17}$)] most of the excess energy (relative to the thermal energy) injected into the photoexcited electrons is quickly transferred to small wave vector LO phonons whose relaxation governs the system cooling for time longer than ~1 ps. The measured dynamics is first dominated by nonequilibrium LO-phonon redistribution in momentum space and then (for $t\geqslant3$ ps) by the anharmonic LO-phonon decay as the nonequilibrium LO phonons approach a thermal distribution. Energy transfers to holes are responsible for the observation of a reduced thermalization time (~1.9 ps) compared to the LO-phonon lifetime. Lattice-temperature-dependent measurements should give additional insight into the energy redistribution processes in polar semiconductors.

*Also with Dipartimento di Elettronica e Informazione, Politecnico di Milano, Piazza Leonardo da Vinci 32, I-20133 Milano, Italy.
†Permanent address: School of Technology, Physics Division, Aristotle University of Thessaloniki, 54006 Thessaloniki, Greece.
‡Permanent address: Istituto di Fisica Medica, Università degli Studi di Bari, Via Orabona 4, I-70126 Bari, Italy.

[1] H. M. van Driel, Phys. Rev. B **19**, 5928 (1979).
[2] W. Pötz and P. Kocevar, Phys. Rev. B **28**, 7040 (1983).
[3] J. H. Collet and T. Amand, J. Phys. Chem. Solids **47**, 153 (1986).
[4] J. Shah, in *Spectroscopy of Nonequilibrium Electrons and Phonons*, edited by C. V. Shank and B. P. Zakharchenya (Elsevier, Amsterdam, 1992), p. 57.
[5] P. Langot, R. Tommasi, and F. Vallée, Solid State Commun. **98**, 171 (1996).
[6] W. Cai, M. C. Marchetti, and M. Lax, Phys. Rev. B **35**, 1369 (1987).
[7] S. E. Kumekov and V. I. Perel', Zh. Eksp. Teor. Fiz. **94**, 346 (1988) [Sov. Phys. JETP **67**, 193 (1988)].
[8] D. von der Linde and R. Lambrich, Phys. Rev. Lett. **42**, 1090 (1979).
[9] K. Leo, W. W. Rühle, and K. Ploog, Phys. Rev. B **38**, 1947 (1988).
[10] U. Hohenester, P. Supancic, P. Kocevar, X. Q. Zhou, W. Kütt, and H. Kurz, Phys. Rev. B **47**, 13 233 (1993).
[11] S. S. Prabhu, A. S. Vengurlekar, S. K. Roy, and J. Shah, Phys. Rev. B **51**, 14 233 (1995).
[12] D. von der Linde, J. Kuhl, and H. Klingenberg, Phys. Rev. Lett. **44**, 1505 (1980).
[13] J. A. Kash and J. C. Tsang, in *Spectroscopy of Nonequilibrium Electrons and Phonons* (Ref. 4), p. 113.
[14] D. Y. Oberli, G. Böhm, and G. Weimann, Phys. Rev. B **47**, 7630 (1993).
[15] P. Brockmann, J. F. Young, P. Hawrylak, and H. M. van Driel, Phys. Rev. B **48**, 11 423 (1993).
[16] K. Vainert, A. Zhukauskas, V. Latinis, and V. Styapankyavichyus, Pis'ma. Zh. Eksp. Teor. Fiz. **47**, 340 (1988) [JETP Lett. **47**, 407 (1988)].
[17] U. Wenschuh, E. Fleiner, and P. Fulde, Phys. Status Solidi B **173**, 221 (1992).
[18] B. Hejda and K. Král, Phys. Rev. B **47**, 15 554 (1993).
[19] A. Zukauskas and S. Jursenas, Phys. Rev. B **51**, 4836 (1995).
[20] V. Klimov, P. Haring Bolivar, and H. Kurz, Phys. Rev. B **52**, 4728 (1995).
[21] P. Lugli, P. Bordone, L. Reggiani, M. Rieger, P. Kocevar, and S. M. Goodnick, Phys. Rev. B **39**, 7852 (1989).
[22] D. S. Kim and P. Y. Yu, Phys. Rev. B **43**, 4158 (1991).
[23] H. Sato and Y. Hori, Phys. Rev. B **36**, 6033 (1987).
[24] M. W. C. Darma Wardana, Phys. Rev. Lett. **66**, 197 (1991).
[25] M. W. C. Darma Wardana, Solid State Commun. **86**, 83 (1993).
[26] X. Q. Zhou, H. M. van Driel, W. W. Rühle, and K. Ploog, Phys. Rev. B **46**, 16 148 (1992).
[27] R. P. Joshi, R. O. Grondin, and D. K. Ferry, Phys. Rev. B **42**, 5685 (1990).
[28] P. Lugli, in *Spectroscopy of Nonequilibrium Electrons and Phonons* (Ref. 4), p. 1.
[29] M. Ulman, D. W. Bailey, L. H. Acioli, F. Vallée, C. J. Stanton, E. P. Ippen, and J. G. Fujimoto, Phys. Rev. B **47**, 10 267 (1993).
[30] J. H. Collet, Phys. Rev. B **39**, 7659 (1989); **47**, 10 279 (1993).
[31] L. Rota and D. K. Ferry, Appl. Phys. Lett. **62**, 2883 (1993).
[32] J. Collet, Phys. Rev. B **47**, 10 279 (1993).
[33] J. Shah, A. Pinczuk, A. C. Gossard, and W. Wiegmann, Phys. Rev. Lett. **54**, 2045 (1985).
[34] R. Tommasi, P. Langot, and F. Vallée, Appl. Phys. Lett. **66**, 1361 (1995).
[35] P. Langot, R. Tommasi, and F. Vallée, Phys. Rev. B **54**, 1775 (1996).
[36] C. K. Sun, H. K. Choi, C. A. Wang, and J. G. Fujimoto, Appl. Phys. Lett. **62**, 747 (1993).

[37] C. L. Tang and D. J. Erskine, Phys. Rev. Lett. **51**, 840 (1983).
[38] J. L. Oudar, D. Hulin, A. Migus, A. Antonetti, and F. Alexandre, Phys. Rev. Lett. **55**, 2074 (1985).
[39] W. Z. Lin, R. W. Schoenlein, J. G. Fujimoto, and E. P. Ippen, IEEE J. Quantum Electron. **24**, 267 (1988).
[40] A slow decay with a time constant of ~1 ns is actually observed which is attributed to carrier recombination. Although it only weakly influences the measured signal for photoexcitation of hot electrons, it has been taken into account when measuring the long term electron cooling.
[41] F. Vallée, Phys. Rev. B **49**, 2460 (1994).